Cover Page

The handle http://hdl.handle.net/1887/43352 holds various files of this Leiden University dissertation.

Author: Velden, D. van der
Title: Mast cell-mediated immune modulation in experimental Rheumatoid Arthritis and Atherosclerosis
Issue Date: 2016-09-29

Chapter 7

Depletion of mast cells in established atherosclerosis increases plaque stability and reduces systemic inflammation in RMB-LDLr^{-/-} mice

Manuscript in preparation

Daniël van der Velden[1,2]

H. Maxime Lagraauw[2]

Hidde Douna[2]

Jacob Amersfoort[1]

René E.M. Toes[1]

Johan Kuiper[2]

Ilze Bot[2]

[1] Department of Rheumatology, Leiden University Medical Center, Leiden, The Netherlands.
[2] Division of Biopharmaceutics, Leiden Academic Centre for Drug Research, Leiden, The Netherlands

Abstract

Objective

Mast cells are potent immune effector cells that are known to contribute to the initiation of atherosclerosis, and are implicated in the destabilization of atherosclerotic lesions matrix degradation via the release of proteases. Furthermore, mast cells can influence T cell skewing via the release of cytokines and cell-cell contact. To study the effects of mast cells on progression of atherosclerosis we used an inducible mast cell knockout mouse, the red mast cell basophil (RMB) mouse, that lacks the LDLr (RMB-LDLr$^{-/-}$). In this novel mouse model mast cells can be depleted after the development of atherosclerotic lesions, which enables us to investigate its effects on atherosclerotic lesion progression.

Methods and Results

We induced atherosclerosis in RMB-LDLr$^{-/-}$ mice by western type diet feeding for 10 weeks. After 10 weeks, a baseline group was sacrificed, while the other groups received either DT to deplete all FcεRIβ^+ cells or PBS as a control. After successful depletion of the mast cells, mice received diet feeding for an additional 6 weeks. No differences were observed in atherosclerotic lesion size between the groups, but a significant increase in collagen content and a reduction in macrophage content and necrotic core area was observed in mast cell depleted mice compared to non-depleted mice. Furthermore, mast cell depletion coincided with a marked reduction in serum IL-6 levels and an increase in IL-10 levels compared to mast cell competent mice. In addition, an increase in regulatory T cells was observed in both the spleen and the heart lymph nodes of mast cell depleted mice.

Conclusions

Mast cell depletion in the progression phase of atherosclerosis improved the lesion stability and reduced systemic inflammation. Besides the well-established role of mast cells in the initial phases of lesion development, this study shows that mast cells also actively contribute to the progression and destabilization of atherosclerosis plaques.

Introduction

Atherosclerosis is a chronic lipid-driven inflammatory disease of the large- and medium sized arteries that involves complex immunologic mechanisms such as accelerated inflammation and reduced tolerance [1]. Next to its involvement in early atherogenesis, the immune system actively contributes to the progression and destabilization of an atherosclerotic plaque. Factors released by activated inflammatory leukocytes such as neutrophils, lipid-laden macrophages, T cells and mast cells result in the loss of matrix components such as collagen and apoptosis of smooth muscle cells, which accelerate the process of plaque destabilization [2]. Frequently, the process of plaque destabilization induces plaque rupture, which leads to acute atherothrombotic occlusion and clinical manifestations such as myocardial infarction and stroke [3]. Activated immune cells, among which mast cells, accumulate in the shoulder region of advanced atherosclerotic lesions, which can trigger matrix degradation by the release of specific proteases [4]. Especially mediators such as tryptase, chymase and histamine that are stored inside the granules of the mast cells are major contributors to plaque destabilization [5]. Circulating tryptase and chymase levels are increased in serum of cardiovascular patients suffering from acute myocardial infarction or unstable angina pectoris compared to patients with stable angina pectoris or healthy controls [6, 7].

To date, a number of experimental atherosclerosis studies have been performed to unravel the contribution of mast cells to atherogenesis and plaque destabilization [8–13]. The mast cell deficient Kit[W-sh/W-sh] mouse strain has been crossed with LDL receptor (LDLr) or ApoE deficient mice and these mice develop smaller and more stable lesions compared to mast cell competent LDLr or ApoE deficient mice [9, 12]. Likewise, systemic mast cell activation by dinitrophenyl (DNP) or compound 48/80 in murine experimental atherosclerosis results in enhanced plaque growth accompanied by features of plaque destabilization such as an increase in intraplaque hemorrhage, macrophage apoptosis and serum tryptase activity, which could be prevented by the mast cell stabilizing drug cromolyn [8, 10]. Specific inhibition of chymase by the use of a protease inhibitor in murine experimental atherosclerosis improves the lesion stability as shown by an increase in collagen content and a decrease in necrotic core area [11]. Although these studies establish the contribution of mast cells to atherogenesis, these studies were performed in Kit[W-sh/W-sh] mice, which are constitutively mast cell deficient and this limits the possibility to study the specific contribution of mast cells to more advanced stages of atherosclerosis. Patients with unstable angina usually have advanced unstable lesions, which underlines the importance to study immune cells such as mast cells in advanced atherosclerotic plaques.

To that aim, we obtained a novel mouse model, the red-basophil-mast cell (RMB) mouse, in which we can study mast cell biology in vivo. In these RMB mice we can efficiently deplete FcεRIβ+-cells (i.e. mast cells and basophils) by injection with diphtheria toxin (DT). Basophils are quite short depleted (<12 days), while a systemic depletion of mast cells

7

is maintained for up to 6 months after the last DT injection [14]. In the current study we induced atherosclerosis in RMB-LDLr$^{-/-}$ mice by western type diet feeding. After lesion induction, the mice received DT to deplete all FcεRIβ$^+$-cells followed by an additional period of diet feeding. At sacrifice, we analyzed lesion size and composition within the aortic root and analyzed systemic parameters such as circulating cytokine levels and blood leukocyte numbers, thereby establishing that mast cells actively contribute to plaque destabilization during the progressive phase of atherosclerosis.

Materials & Methods

Mice

All animal work was performed conform the guidelines from the Directive 2010/63/EU of the European Parliament. Experiments were approved by the Leiden University Animal Ethics committee. The red mast cell and basophil mouse strain (RMB mice, official name: B6.Ms4a2^{tm1Mal}) was provided by the laboratory of dr. P. Launay, INSERM U1149, Paris, France [14]. These mice express the simian diphtheria toxin receptor under control of the promoter of the FcεRIβ gene. Injection of diphtheria toxin will therefore induce apoptosis of all FcεRIβ expressing cells (mast cells and basophils). RMB mice were crossed with LDLr$^{-/-}$ mice (The Jackson Laboratory, USA) to obtain atherosclerosis-prone RMB-LDLr$^{-/-}$ mice. LDLr$^{-/-}$ mice were included in the study as a control for DT-mediated side effects [15, 16].

To study the effects of mast cell depletion on established atherosclerosis (Figure 1a), RMB-LDLr$^{-/-}$ mice (7-10 weeks old) were fed a Western type diet (0.25% cholesterol and 15% cacao butter, SDS, Sussex, UK) for 10 weeks to induce atherosclerosis. At week 10, a subset of mice was sacrificed as baseline control, while the remaining mice received either DT injections to deplete FcεRIβ$^+$ cells or PBS as a control. To systemically deplete all FcεRIβ$^+$ cells, mice were injected i.p. for three times every other day with 25 ng/g bodyweight DT (Diphtheria Toxin Unnicked, C. diphtheriae (Cat #322326), CalBiochem, US). Efficiency of DT treatment was determined by both FACS analysis for circulating basophils (CD49b$^+$/FcεRI$^+$/IgE$^+$) three days after the last DT injection and by a mast cell staining (chloro-acetate esterase (CAE), Sigma-Aldrich, US) of the aortic root at the end of the study. At sacrifice, mice were anaesthetized and sacrificed via orbital exsanguination. Fixation through the left cardiac chamber was performed with phosphate-buffered saline (PBS). Subsequently, the heart was excised and stored in 3.7% neutral-buffered formalin (Formal-fixx; Shandon Scientific Ltd, UK) for 18 hours at 4°C for histological analysis. Serum was collected to determine circulating cytokine levels. Splenocytes, EDTA-blood and heart lymph nodes were isolated for flow cytometry analysis of common leukocyte populations.

Histology and morphometry

After fixation, hearts were embedded in Tissue-Tek® O.C.T.™ compound (Sakura BV, The Netherlands) after which 10 μm cryosections were prepared using a Leica CM3050S cryostat and stained with Oil-Red-O (Sigma-Aldrich, US).

Oil-Red-O-stained sections were used to determine lesion size (in μm^2) in the aortic root. Mean lesion area (in μm^2) was calculated from 6 consecutive sections, starting at the appearance of the tricuspid valves. A CAE staining was performed to visualize mast cells, which were in a blinded manner counted manually by an independent operator. Collagen content was determined in corresponding sections by staining with Masson's

Trichrome staining (Sigma-Aldrich, US). Macrophages were visualized with an immunohistochemical staining using a primary rat anti-mouse macrophages/monocytes antibody (Clone moma-2, isotype IgG2b, 1:1000, Cat# MCA519G, AbD Serotec, Germany), while a goat anti-rat alkaline phosphatase (1:500, Cat# A8438 Sigma Aldrich, US) was used as a secondary antibody and nitro blue tetrazolium and 5-bromo-4-chloro-3-indolyl phosphate as enzyme substrates.

The atherosclerotic lesion areas and histological stainings of the aortic root cryosections were quantified using the Leica image analysis system, consisting of a Leica DMRE microscope coupled to a video camera and Leica Qwin Imaging analysis system (Leica Ltd, UK). The percentage of collagen and macrophages in the lesions was determined by dividing the collagen- or MOMA-2 positive area by the total lesion surface area. The necrotic core size was defined as the a-cellular, debris-rich plaque area and represented as percentage of the total plaque area and measured in collagen stained sections.

Serum analysis

Serum concentrations of total cholesterol was determined by enzymatic colorimetric assay according to protocol of supplier (Roche Diagnostics, Switzerland). Precipath (Standardized serum Roche Diagnostics, US) was used as internal standard. Cytokine levels in serum were determined using a commercially available ELISA kit (Becton Dickinson, US). All procedures were according to manufacturer's protocol.

Flow cytometry

At sacrifice, blood was obtained in EDTA tubes and erythrocytes were removed using a specific erythrocyte lysis buffer (0.15 M NH_4Cl, 10 mM $NaHCO_3$, 0.1 mM EDTA, pH 7.3).

Blood leukocytes were stained extracellularly to determine a) monocytes ($NK1.1^-/Ly6G^-/CD11b^{hi}$), inflammatory monocytes ($NK1.1^-/Ly6G^-/CD11b^{hi}/Ly6C^{hi}/CCR2^+$) and neutrophils ($NK1.1^-/Ly6G^{hi}/CD11b^{hi}$), b) basophils ($CD3^-/CD4^-/CD19^-/CD8^-/CD49b^+/IgE^+/CD117^-$), c) T cells ($CD3^+/CD4^+$) and d) B cells ($CD19^+/B220^+$). The antibodies used (eBiosciences, US) are summarized in table 1. Flow cytometry analysis was performed on the FACSCantoII and data were analyzed using FACSDiva software (Becton Dickinson, US).

7

Table 1: Antibody panels used for flow cytometry analysis

Staining	FITC	PE	PerCP	APC	e-Fluor-450
A.	NK1.1 (Clone: PK136)	Ly6G (Clone: 1A8)	Ly6C (Clone: HK1.4)	CCR2 (Clone: 475301)	CD11b (Clone: M1/70)
B.	IgE (Clone: R35-72)	IgE (Clone: R35-72)	CD3/4/19/8 (dump channel)	CD49b (Clone: HMa2)	n/a
C.	CD44 (Clone: IM7)	CCR7 (Clone: 4B12)	CD8α (Clone: 53-6.7)	CD62L (Clone: MEL-14)	CD4 (Clone: GK1.5)
D.	IgM (Clone: II/41)	CD45RA (Clone: RA3-6B2)	CD19 (Clone: eBio1D3)	IgD (Clone: 11-26c)	CD5 (Clone: 53-7.3)

Stimulation of splenocytes and heart lymph nodes

At sacrifice, single cell suspensions were prepared from the spleen and heart lymph nodes by using a 70 μm cell strainer (Falcon, US). Erythrocytes were removed using a specific erythrocyte lysis buffer (0.15 M NH_4Cl, 10 mM

NaHCO$_3$, 0.1 mM EDTA, pH 7.3).

Regulatory T cell numbers were determined by staining with with eFluor-450 conjugated rat anti mouse CD4. Next, cells were fixed and permeabilized according to supplier's protocol (eBiosciences, US). Subsequently, cells were stained with APC conjugated rat anti-mouse/human FoxP3 or corresponding isotype as a control (eBioscience, US).

To determine inflammatory T cell phenotypes in spleen or lymph nodes, 400.000 cells/well were cultured in 96 well round-bottom plates (Greiner Bio-One, The Netherlands) and stimulated with anti-CD3 and anti-CD28 (2 µg/mL each, eBioscience, US) in complete IMDM, supplemented with 10% hiFCS, 100 u/mL penicillin/streptomycin, 2 mM L-Glutamine (PAA, Austria) and 20 mM β-mercaptoethanol (Sigma-Aldrich, US). After 1 hour, brefeldin A (Sigma-Aldrich, US) was added up to a concentration of 10 µg/mL to inhibit protein transport to the outside of the cell. After an additional 4 hours of culture, cells were washed twice with FACS Buffer (PBS, 1% BSA, 2mM EDTA) and stained for T cell surface markers.

Cells were first stained with eFluor-450 conjugated rat anti mouse CD4. Next, cells were fixed and permeabilized according to supplier's protocol (eBiosciences, The Netherlands), followed by intracellular staining with FITC conjugated rat anti-mouse IFNγ, PE conjugated rat anti-mouse IL-17 and APC conjugated rat anti-mouse IL-10 or corresponding isotypes as a control (eBioscience, The Netherlands). Flow cytometry analysis was performed as described above.

Statistical analysis

Values are expressed as mean ± SEM. Data of three groups were analyzed using a one-way ANOVA. Statistical analysis was performed using Graphpad Prism. Probability values of $P<0.05$ were considered significant.

Results

Body weight, total cholesterol and mast cell depletion

To study the contribution of mast cells to plaque progression, we induced atherosclerosis in RMB-LDLr$^{-/-}$ mice by feeding a western-type diet for 10 weeks, after which we depleted FcεRIβ$^+$-cells using DT (Fig. 1a). Three days after the last DT injection, we performed FACS analysis on blood samples for basophils as a control for depletion efficiency of DT. We detected basophils in both the PBS treated RMB-LDLr$^{-/-}$, whereas basophils were completely absent in the DT treated RMB-LDLr$^{-/-}$ group (Fig. 1b). After depletion of FcεRIβ$^+$-cells, all mice received an additional diet feeding for 6 weeks. At sacrifice, we observed a difference in body weight gain between the DT and PBS treated mice (Suppl. Fig. 1a), caused by the DT treatment as the DT treated LDLr$^{-/-}$ controls showed a similar weight curve as DT treated RMB-LDLr$^{-/-}$ mice. Further analysis showed no differences in total plasma cholesterol levels (Suppl. Fig. 1b) and total lesion size in the aortic root between DT treated LDLr$^{-/-}$ controls or RMB-LDLr$^{-/-}$ mice (Suppl. Fig. 1c). In addition, DT treatment did not result in differences in total leukocyte count and percentage of different circulating leukocytes (Suppl. Fig. 1d). Mast cells were detected in the aortic root of PBS treated RMB-LDLr$^{-/-}$, while significant depletion of mast cells was observed in DT treated mice (Fig. 1d). We also observed a complete depletion of mast cells in the skin upon DT treatment of RMB-LDLr$^{-/-}$ mice (data not shown).
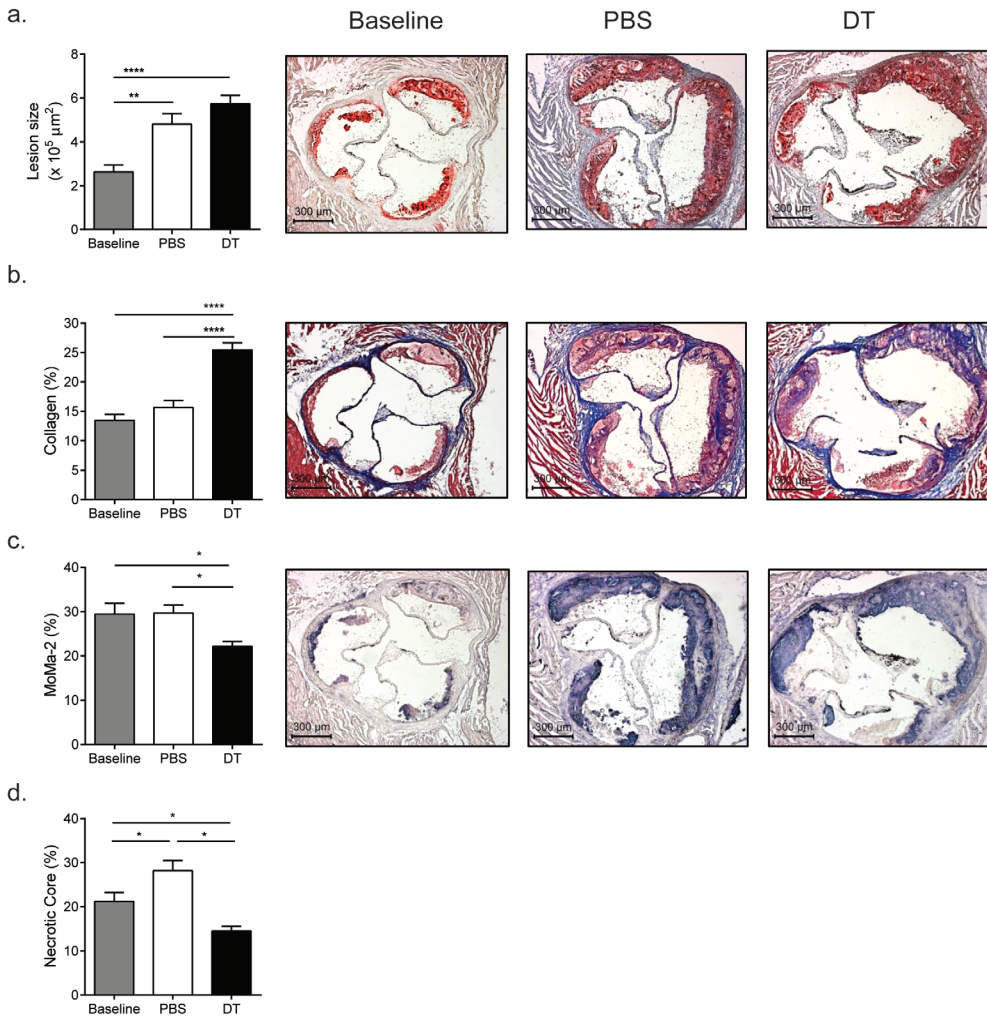
Figure 1. Study outline and basic characteristics in RMB-LDLr$^{-/-}$ and LDLr$^{-/-}$ mice.
(A) Flow-chart of the in vivo experimental set-up. (B) Representative FACS plots of basophil gating in PBS and DT treated mice and summary of all mice. (C) Serum total cholesterol levels from all groups (n=15/group). (D) Perivascular mast cell count in the aortic root of PBS or DT injected RMB-LDLr$^{-/-}$ and LDLr$^{-/-}$ mice (n=15/group). Arrows in magnification point to perivascular mast cells. **P<0.01 ****P<0.0001.

7

Histological analysis of the aortic root

Next, we performed histological analysis of the aortic root to determine atherosclerotic lesion size and composition. Quantification of the lesion size in Oil-Red-O stained sections showed that the mean lesion size increased in both PBS and DT treated RMB-LDLr$^{-/-}$ mice, with 82% and 118% respectively, compared to baseline values (Fig. 2a). We did not detect any differences in mean lesion size between PBS and DT treated mice as depicted in figure 2a. The collagen content was significantly elevated in FcεRIβ^{+}-cell depleted mice compared to both the baseline value (DT: 25.4 ± 1.2 % versus Baseline: 13.5 ± 1.0 %, p < 0.0001) and the value in PBS treated mice (DT: 25.4 ± 1.2 % versus PBS: 15.6 ± 1.2 %, p < 0.0001, Fig. 2b). Furthermore, we observed a significant reduction in macrophage positive area (DT: 22.2 ± 1.1 % versus PBS: 29.7 ± 1.8 %, p < 0.001) and percentage of necrotic core area (DT: 14.5 ± 4.6 % versus PBS: 28.2 ± 9.7 %, p < 0.001) in FcεRIβ^{+}-cell depleted RMB-LDLr$^{-/-}$ mice compared to non FcεRIβ^{+}-cell depleted RMB-LDLr$^{-/-}$ mice (Fig. 2c-d).

Figure 2. Depletion of FcεRIβ⁺ cells in RMB-LDLr⁻ᐟ⁻ mice does not influence plaque progression but increases lesion stability in the aortic root.
(A) Depletion of FcεRIβ⁺ cells did not influenced the plaque size in DT injected RMB-LDLr⁻ᐟ⁻ mice compared to PBS treated. Compared to non-depleted mice, depletion of FcεRIβ⁺-cells during lesion progression coincided with an increase in collagen content as determined with Masson's Trichrome staining (B) as well as a reduction in macrophage content as determined by MOMA-2 staining (C) and a reduction in necrotic core (D) as percentage total lesion size (n=15/group). Representative cross-sections stained with Oil-Red-O and haematoxylin, Masson's Trichrome staining and MOMA-2 are shown. **P<0.01, ****P<0.0001.

Systemic cytokine profile in RMB-LDLr$^{-/-}$ mice

We analyzed the serum for proatherogenic cytokines such as IL-6, MCP-1, TNFα, IFNγ, IL-17 and the atheroprotective cytokine IL-10. As depicted in figure 3, no differences were detected in TNFα, IFNγ and IL-17 levels. Interestingly, we observed a significant increase in the chemokine MCP-1 level in the non-FcεRIβ$^+$-cell depleted mice compared to baseline values which was not observed in the FcεRIβ$^+$-cell depleted group. Furthermore, a significant increase in serum IL-10 was detected in FcεRIβ$^+$-cell depleted mice compared to baseline values (DT: 512.2 ± 51.3 versus Baseline: 275.7 ± 19.6 pg/mL, p=0.0005) and non-depleted mice (DT: 512.2 ± 51.3 versus PBS: 357.4 ± 40.2 pg/mL, p=0.02) (Fig. 3). In addition, we observed a marked reduction in circulating IL-6 in FcεRIβ$^+$-cell depleted mice compared to baseline values (DT: 124.5 ± 13.8 versus Baseline: 234.3 ± 12.8 pg/mL, p=0.0005) and non-depleted mice (DT: 124.5 ± 13.8 versus PBS 210.7 ± 20.3 pg/mL, p=0.005) (Fig. 3). DT injection in LDLr$^{-/-}$ mice did not influence cytokine levels (Suppl. Fig 1e).
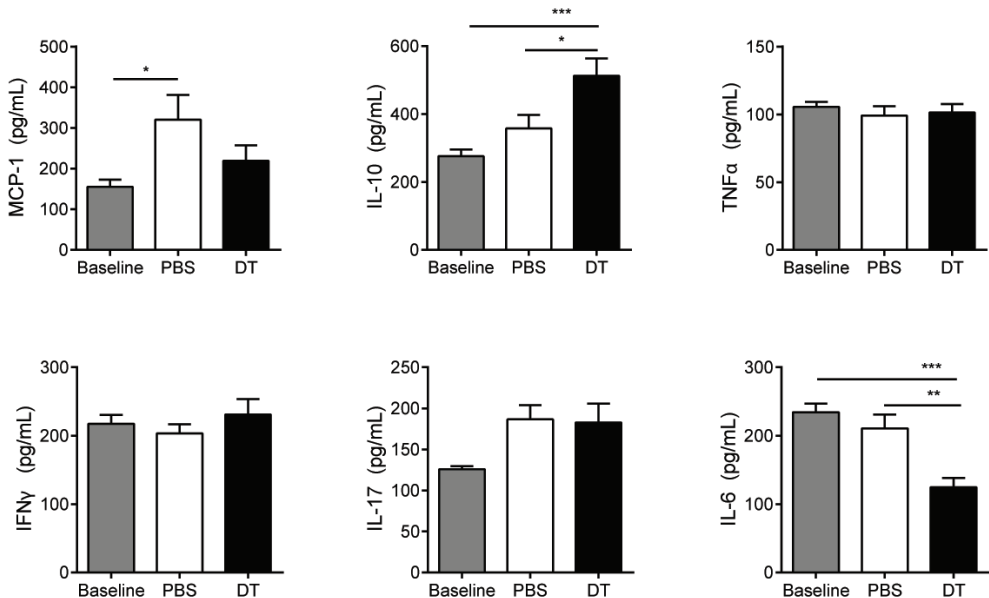
Figure 3. Increased levels of atheroprotective IL-10 and decreased levels of atherogenic MCP-1 and IL-6 after depletion of FcεRIβ$^+$ cells in RMB-LDLr$^{-/-}$ mice.
Serum levels of IL-6, MCP-1, TNFα, IFNγ, IL-17 and IL-10 were quantified in serum of all groups (n=15/group). *P<0.05, ***P<0.001.

Flow cytometry analysis

At sacrifice, flow cytometry analysis of the blood for leukocyte populations showed a complete repopulation of basophils in DT treated RMB-LDLr$^{-/-}$ mice (Fig. 4). Although we did not observe a difference in the percentage of total monocyte levels between groups, the percentage of inflammatory monocytes were significantly reduced in DT treated mice. No differences were observed between groups for other leukocyte subsets such as neutrophils, T cells and B cells.
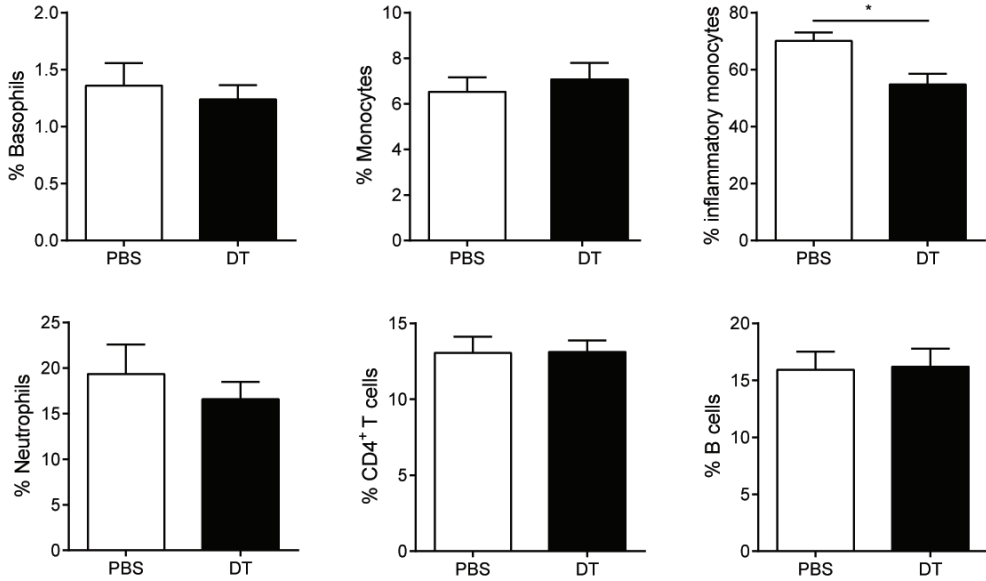

Figure 4. Flow cytometry analysis of circulating blood leukocytes showed a reduction in inflammatory monocytes in FcεRIβ+ cell depleted mice.
No differences were detected in circulating blood basophils, monocytes, neutrophils, CD4+ T cells and B cells. The percentage of inflammatory monocytes in FcεRIβ+-cell depleted mice was reduced compared to non-depleted mice. *P<0.05.

In both the spleen and the lymph nodes draining from the heart we performed flow cytometry analysis to determine the percentages of T cell subsets. As depicted in figure 5a, we did not observe any difference in total CD4$^+$ T cells or proatherogenic phenotypes such as IL-17$^+$ (T$_h$17) and IFNγ^+ CD4$^+$ (T$_h$1) T cells in the both spleen and heart lymph nodes. Atheroprotective regulatory T cells were measured in spleen and heart lymph node. Analysis showed a significant increase in CD4$^+$/FoxP3$^+$ regulatory T cell levels in both the spleen (DT 10.0 ± 0.4 % versus PBS 7.6 ± 0.3 %, p=0.0002) and heart lymph nodes (DT: 9.9 ± 0.7 % versus PBS: 7.8 ± 0.5 %, p=0.02) of FcϵRIβ^+-cell depleted mice compared to non-depleted mice (Fig. 5b). In addition, we did not observe any differences in T cell subsets in DT treated LDLr$^{-/-}$ mice (Suppl. Fig. 1f, g). Figure 5c shows representative FACS plots of the FoxP3 staining within the CD4$^+$ population of the heart lymph nodes.
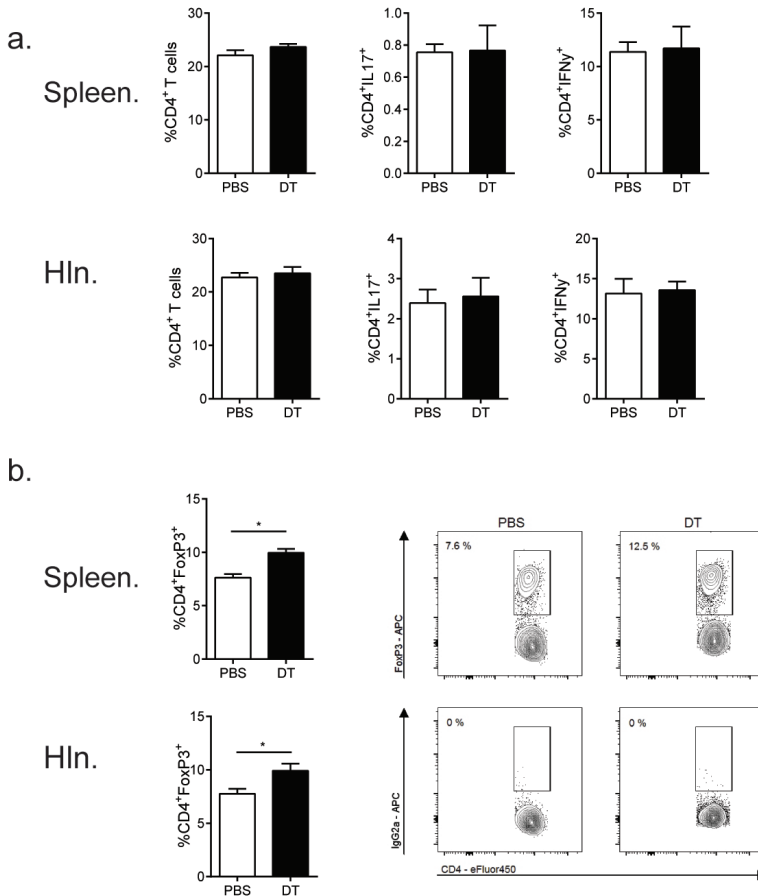
Figure 5. T cell phenotype in spleen and heart lymph nodes showed an increase in regulatory T cells in FcϵRIβ^+ cells depleted mice.
(A) Analysis of both stimulated splenocytes and heart lymph node cells showed no differences in atherogenic T cell phenotypes. (B) A slight but significant increase in regulatory T cell was detected in splenocytes and heart lymph node cells of depleted mice compared to non-depleted mice. (C) Representative FACS plots are shown for all groups. *P<0.05.

Discussion

The major underlying cause of an acute cardiovascular syndrome (ACS) is the rupture of an unstable atherosclerotic lesion, which leads to ischemia in the distal tissue resulting in clinical symptoms such as a myocardial infarction or a stroke. Plaque destabilization is an important phase that precedes plaque rupture and mast cells can actively contribute to that process by the release of proteases such as tryptase, chymase and matrix metalloproteinases (MMPs), which induce apoptosis of collagen producing smooth muscle cells and degrade the extracellular matrix of the lesion. Indeed, in a number of studies elevated levels of the mast cell specific proteases tryptase and chymase have been reported in the serum of ACS patients compared to non-ACS patients and have been shown to correlate with plaque vulnerability and clinical outcome [17–19]. Additionally, in a recent study by Willems et al. the number of intraplaque mast cells was determined in lesions obtained from patients undergoing carotid endarterectomy. The number of lesional mast cells and serum tryptase levels was significantly higher in patients that had a secondary cardiovascular event compared to patients that remained asymptomatic during follow-up of the study [20]. These data indicate that mast cell numbers in the lesion are associated with future cardiovascular events and one suggest that mast cells indeed contribute to lesion destabilization that can lead to plaque rupture. To further study the effects of mast cells in the progressive phase of atherosclerosis, we made use of a mast cell inducible knockout mouse model on an atherosclerotic prone background (RMB-LDLr$^{-/-}$ mouse). This model enables us to study the contributions of mast cells beyond their role in the initial phases of atherosclerosis.

Our current study shows that absence of mast cells during lesion progression did not affect lesion size, but did result in an increased plaque stability and a reduction in the systemic inflammatory response. Our data are in line with a recent study from Wang et al., where pharmacological stabilization of mast cells in established atherosclerosis in LDLr$^{-/-}$ mice by the use of the drug cromolyn results in a reduced inflammatory plaque phenotype [13]. Similar to our data, mast cell stabilization reduces plaque macrophage content, but unlike their study we did not observe a reduction in plaque size and plasma cholesterol levels in mast cell depleted compared to non-depleted mice. One explanation could be the specificity of cromolyn in mice, which is subject of debate [21]. Cromolyn has been reported to interact with ubiquitous proteins such as G-protein-coupled receptor 35 (GPR35), which are highly expressed in different (non)-immune cells and tissues as in the colon, spleen, monocytes, T cells, neutrophils and dendritic cells [22, 23]. Therefore, one could speculate that cromolyn is able to influence more cellular processes besides the stabilizing effect on mast cells, which could have been contributed to the observed effects on lesion size in cromolyn treated mice [24]. Nonetheless, it can be concluded that mast cell depletion or stabilization increases lesion stability, which can be caused by a reduced release of mediators that induce plaque destabilization. For example, in the atherosclerotic lesion the majority of mast cells expresses the extracellular matrix

degrading enzyme chymase [25]. Activation of mast cells leads to the release of mediators such as chymase, which results in the breakdown of collagen, degradation of HDL and in apoptosis of smooth muscle cells [26].

Mast cells secrete chemokines and cytokines that can attract other immune cells into the lesion and MCP-1 is an important chemokine in the recruitment of inflammatory monocytes into the atherosclerotic lesion [27, 28]. Compared to baseline values, PBS treated RMB-LDLr$^{-/-}$ mice but not mast cell depleted RMB-LDLr$^{-/-}$ mice showed a significant increase in serum MCP-1 concentrations after six weeks of additional diet. Furthermore, we detected a significant reduction in circulating inflammatory monocytes in mast cell depleted RMB-LDLr$^{-/-}$ mice. Together with the reduction of the chemokine MCP-1 levels this could this explain, to a certain extent, the reduction in macrophage positive area observed in mast cell depleted mice.

Pathogenic (T$_h$1 and T$_h$17) and protective regulatory T cells (Tregs) are tightly balanced during immune responses. This balance is controlled by cytokines, e.g. IL-12, IL-4 and IL-6, and cell-cell interactions via co-stimulatory molecules like CD80/86, ICOSL, CD40 and OX40L, which are expressed by antigen-presenting cells such as dendritic cells. Mast cells are efficient effector immune cells that upon activation by various ligands actively secrete potent mediators, such as IL-8, TNFα and IL-6, and on top of that also express co-stimulatory molecules such as CD80/86 and OX40L that are able to directly interact with T cells thereby enhancing the proliferation and function of T cells [29–33]. In our current study we were unable to detect any differences in atherogenic T cell phenotypes such as T$_h$1 and T$_h$17 T cells between the groups. This could be due to the fact that in established lesions the adaptive immune response has already fully developed and therefore mast cell depletion is unable to significantly alter this established atherogenic T cell phenotypes. In contrast, mast cell depletion coincided with an increase in Tregs in both the spleen and the draining heart lymph nodes and elevated serum levels of IL-10. Tregs are essential in the dampening of immune responses in inflammatory conditions during atherosclerosis by the secretion of anti-inflammatory TGFβ and IL-10 [34]. Mast cells have been shown to directly inhibit Tregs functions via the co-stimulatory molecule OX40-OX40L, the release of histamine and secretion of IL-6 [33, 35, 36].

The acute phase cytokine IL-6 is a key cytokine in the skewing of naïve T cells towards T$_h$17 cells and inhibition of Treg development [37–39]. Under inflammatory conditions, IL-6 producing mast cells co-localize with Tregs and T$_h$17 cells in the draining lymph node of immunized mice in an experimental model of multiple sclerosis and appear to play an important role in the promotion of T$_h$17 cell differentiation and inhibiting Treg suppression [35]. Especially the interaction of the co-stimulatory molecules OX40L and OX40 between mast cells and Tregs, respectively, has been shown to block the function of Tregs and promote T$_h$17 cell differentiation [35]. T$_h$17 cells have been implicated in the pathogenesis of murine and human atherosclerosis [40]. In our current study, we observed a reduction of IL-6 and an increase in IL-10 in the serum of mast cell depleted mice compared to

7

non-depleted mice. Most likely, this reduction in IL-6 positively influenced the T cell homeostasis in favor of IL-10 producing Tregs.

In conclusion, here we show that a systemic mast cell depletion in RMB-LDLr^{-/-} mice with established atherosclerotic lesions locally affects plaque phenotype but also systemically alters cytokine profile and T cell phenotype. Together with observation that intraplaque mast cell numbers correlate with clinical outcome, these data indicate that mast cell stabilization in cardiovascular patients with unstable atherosclerotic lesions could be beneficial in preventing lesion destabilization.

References

1. Hansson GK, Hermansson A (2011) The immune system in atherosclerosis. Nat Immunol 12:204–212

2. Silvestre-Roig C, Winther MP de, Weber C, Daemen MJ, Lutgens E, Soehnlein O (2014) Atherosclerotic Plaque Destabilization Mechanisms, Models, and Therapeutic Strategies. Circ Res 114:214–226

3. Libby P (2013) Mechanisms of Acute Coronary Syndromes and Their Implications for Therapy. N Engl J Med 368:2004–2013

4. Kaartinen M, Penttilä A, Kovanen PT (1994) Accumulation of activated mast cells in the shoulder region of human coronary atheroma, the predilection site of atheromatous rupture. Circulation 90:1669–1678

5. Wernersson S, Pejler G (2014) Mast cell secretory granules: armed for battle. Nat Rev Immunol 14:478–494

6. He A, Shi G-P (2013) Mast Cell Chymase and Tryptase as Targets for Cardiovascular and Metabolic Diseases. Curr Pharm Des 19:1114–1125

7. Bot I, Shi G-P, Kovanen PT (2015) Mast Cells as Effectors in Atherosclerosis. Arterioscler Thromb Vasc Biol 35:265–271

8. Bot I, de Jager SCA, Zernecke A, Lindstedt KA, van Berkel TJC, Weber C, Biessen EAL (2007) Perivascular mast cells promote atherogenesis and induce plaque destabilization in apolipoprotein E-deficient mice. Circulation 115:2516–2525

9. Sun J, Sukhova GK, Wolters PJ, Yang M, Kitamoto S, Libby P, MacFarlane LA, Clair JM-S, Shi G-P (2007) Mast cells promote atherosclerosis by releasing proinflammatory cytokines. Nat Med 13:719–724

10. Tang Y, Yang Y, Wang S, Huang T, Tang C, Xu Z, Sun Y (2009) Mast cell degranulator compound 48-80 promotes atherosclerotic plaque in apolipoprotein E knockout mice with perivascular common carotid collar placement. Chin Med J (Engl) 122:319–325

11. Bot I, Bot M, van Heiningen SH, et al (2011) Mast cell chymase inhibition reduces atherosclerotic plaque progression and improves plaque stability in ApoE^{-/-} mice. Cardiovasc Res 89:244–252

12. Smith DD, Tan X, Raveendran VV, Tawfik O, Stechschulte DJ, Dileepan KN (2012) Mast cell deficiency attenuates progression of atherosclerosis and hepatic steatosis in apolipoprotein E-null mice. Am J Physiol - Heart Circ Physiol 302:H2612–H2621

13. Wang J, Sjöberg S, Tia V, Secco B, Chen H, Yang M, Sukhova GK, Shi G-P (2013) Pharmaceutical stabilization of mast cells attenuates experimental atherogenesis in low-density lipoprotein receptor-

deficient mice. Atherosclerosis 229:304–309

14. Dahdah A, Gautier G, Attout T, et al (2014) Mast cells aggravate sepsis by inhibiting peritoneal macrophage phagocytosis. J Clin Invest 124:4577–4589

15. Chapman TJ, Georas SN (2013) Adjuvant effect of diphtheria toxin after mucosal administration in both wild type and diphtheria toxin receptor engineered mouse strains. J Immunol Methods 400–401:122–126

16. Meyer zu Hörste G, Zozulya AL, El-Haddad H, Lehmann HC, Hartung H-P, Wiendl H, Kieseier BC (2010) Active immunization induces toxicity of diphtheria toxin in diphtheria resistant mice — Implications for neuroinflammatory models. J Immunol Methods 354:80–84

17. Deliargyris EN, Upadhya B, Sane DC, Dehmer GJ, Pye J, Smith SC, Boucher WS, Theoharides TC (2005) Mast cell tryptase: a new biomarker in patients with stable coronary artery disease. Atherosclerosis 178:381–386

18. Filipiak KJ, Tarchalska-Krynska B, Opolski G, Rdzanek A, Kochman J, Kosior DA, Czlonkowski A (2003) Tryptase levels in patients after acute coronary syndromes: The potential new marker of an unstable plaque? Clin Cardiol 26:366–372

19. Xiang M, Sun J, Lin Y, Zhang J, Chen H, Yang D, Wang J, Shi G-P (2011) Usefulness of Serum Tryptase Level as an Independent Biomarker for Coronary Plaque Instability in a Chinese Population. Atherosclerosis 215:494–499

20. Willems S, Vink A, Bot I, et al (2013) Mast cells in human carotid atherosclerotic plaques are associated with intraplaque microvessel density and the occurrence of future cardiovascular events. Eur Heart J 34:3699–3706

21. Oka T, Kalesnikoff J, Starkl P, Tsai M, Galli SJ (2012) Evidence questioning cromolyn's effectiveness and selectivity as a "mast cell stabilizer" in mice. Lab Invest 92:1472–1482

22. Yang Y, Lu JY-L, Wu X, Summer S, Whoriskey J, Saris C, Reagan JD (2010) G-protein-coupled receptor 35 is a target of the asthma drugs cromolyn disodium and nedocromil sodium. Pharmacology 86:1–5

23. Wang J, Simonavicius N, Wu X, Swaminath G, Reagan J, Tian H, Ling L (2006) Kynurenic Acid as a Ligand for Orphan G Protein-coupled Receptor GPR35. J Biol Chem 281:22021–22028

24. MacKenzie A, Lappin J, Taylor D, Nicklin S, Milligan G (2011) GPR35 as a novel therapeutic target. Mol Struct Endocrinol 2:68

25. Jeziorska M, McCOLLUM C, Woolley DE (1997) Mast Cell Distribution, Activation, and Phenotype in Atherosclerotic Lesions of Human Carotid Arteries. J Pathol 182:115–122

26. Kovanen PT (2007) Mast cells and degradation of pericellular and extracellular matrices: potential contributions to erosion, rupture and intraplaque haemorrhage of atherosclerotic plaques. Biochem Soc Trans 35:857–861

27. Boring L, Gosling J, Cleary M, Charo IF (1998) Decreased lesion formation in CCR2-/- mice reveals a role for chemokines in the initiation of atherosclerosis. Nature 394:894–897

28. Geissmann F, Jung S, Littman DR (2003) Blood Monocytes Consist of Two Principal Subsets with Distinct Migratory Properties. Immunity 19:71–82

29. Nakae S, Suto H, Kakurai M, Sedgwick JD, Tsai M, Galli SJ (2005) Mast cells enhance T cell activation: Importance of mast cell-derived TNF. Proc Natl Acad Sci U S A 102:6467–6472

30. Galli SJ, Nakae S, Tsai M (2005) Mast cells in the development of adaptive immune responses.

7

Nat Immunol 6:135–142

31. Kashiwakura J, Yokoi H, Saito H, Okayama Y (2004) T cell proliferation by direct cross-talk between OX40 ligand on human mast cells and OX40 on human T cells: comparison of gene expression profiles between human tonsillar and lung-cultured mast cells. J Immunol Baltim Md 1950 173:5247–5257

32. Frandji P, Tkaczyk C, Oskeritzian C, David B, Desaymard C, Mécheri S (1996) Exogenous and endogenous antigens are differentially presented by mast cells to CD4+ T lymphocytes. Eur J Immunol 26:2517–2528

33. Bulfone-Paus S, Bahri R (2015) Mast cells as regulators of T cell responses. Immunol Mem 394

34. Sakaguchi S, Yamaguchi T, Nomura T, Ono M (2008) Regulatory T Cells and Immune Tolerance. Cell 133:775–787

35. Piconese S, Gri G, Tripodo C, Musio S, Gorzanelli A, Frossi B, Pedotti R, Pucillo CE, Colombo MP (2009) Mast cells counteract regulatory T-cell suppression through interleukin-6 and OX40/OX40L axis toward Th17-cell differentiation. Blood 114:2639–2648

36. Forward NA, Furlong SJ, Yang Y, Lin T-J, Hoskin DW (2009) Mast cells down-regulate CD4+CD25+ T regulatory cell suppressor function via histamine H1 receptor interaction. J Immunol Baltim Md 1950 183:3014–3022

37. Gabay C (2006) Interleukin-6 and chronic inflammation. Arthritis Res Ther 8 Suppl 2:S3

38. Romano M, Sironi M, Toniatti C, et al (1997) Role of IL-6 and Its Soluble Receptor in Induction of Chemokines and Leukocyte Recruitment. Immunity 6:315–325

39. Kimura A, Kishimoto T (2010) IL-6: regulator of Treg/Th17 balance. Eur J Immunol 40:1830–1835

40. Taleb S, Tedgui A, Mallat Z (2015) IL-17 and Th17 Cells in Atherosclerosis Subtle and Contextual Roles. Arterioscler Thromb Vasc Biol 35:258–264
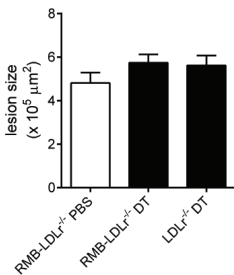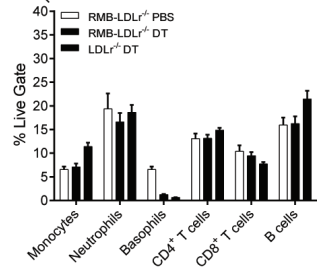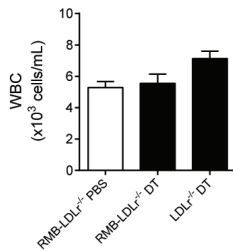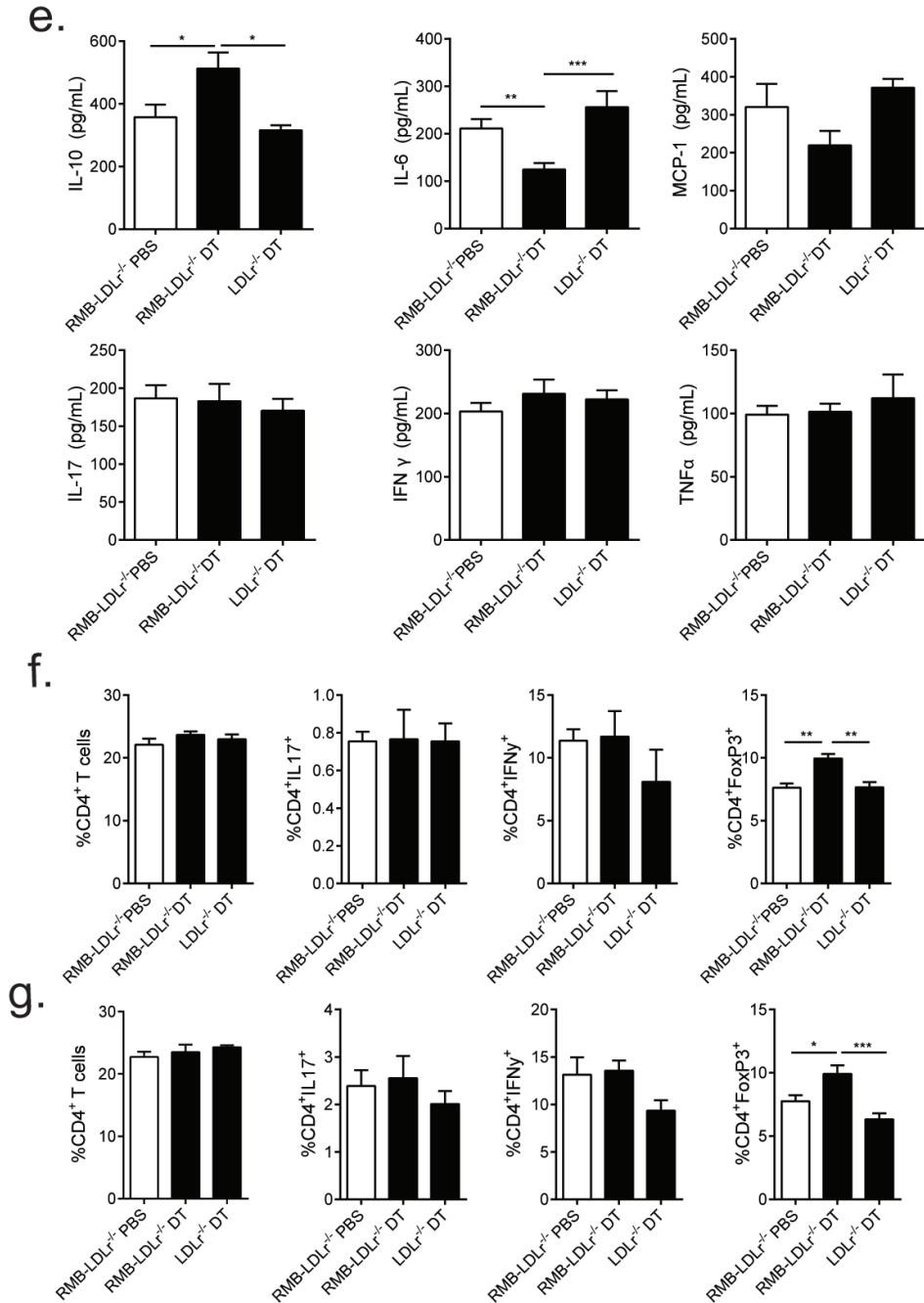
Supplemental data
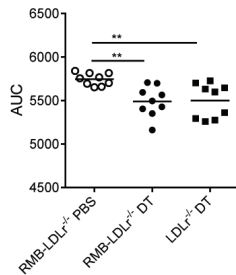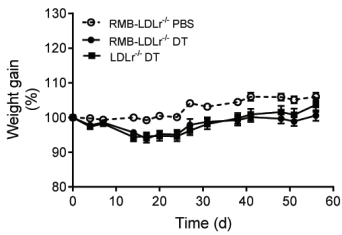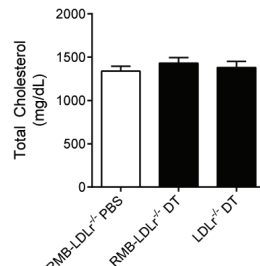
Supplemental figure 1: DT treatment of LDLr$^{-/-}$ mice as control for DT off-target effects
(A) Body weight of RMB-LDLr$^{-/-}$ and LDLr$^{-/-}$ mice injected with either PBS or DT (n=15/group). Total plasma cholesterol levels (B), total lesion size (C), total WBC and leukocyte subsets (D), cytokine levels (E), T cell subsets in hLN (F) and T cell subsets in spleen (G) of PBS and DT treated RMB-LDLr$^{-/-}$ and DT treated LDLr$^{-/-}$ mice (n=15/group). *P<0.05, **P<0.01, ***P<0.001.